Polymer Bulletin (2020) 77:6213–6226
https://doi.org/10.1007/s00289-019-03068-4

ORIGINAL PAPER

TEMPO-oxidized cellulose nanofibers/TiO_2 nanocomposite as new adsorbent for Brilliant Blue dye removal

Zehbah Ali Al-Ahmed[1] · Abeer A. Hassan[2] · Sahar M. El-Khouly[3] · Shaymaa E. El-Shafey[3]

Received: 14 June 2019 / Revised: 3 October 2019 / Accepted: 10 December 2019 /
Published online: 19 December 2019

Abstract
In this article, TEMPO-oxidized cellulose nanofiber (TEMPO-CNF) prepared from bagasse was described and utilized as a sustainable material for the preparation of new nanocomposites. TiO_2 nanoparticles were synthesized by in situ precipitation in the presence of TEMPO-CNF. The prepared nanocomposite, TEMPO-CNF/TiO_2, was characterized by using FT-IR, XRD, TGA, SEM, and EDX analysis. The results proved that homogenous spherical TiO_2 nanoparticles were formed with the particles of TEMPO-CNF. TEMPO-CNF/TiO_2 nanocomposite was examined as an adsorbent for Brilliant Blue (BB) adsorption. The highest BB removal efficiency was observed at pH 7, the adsorption process is well described by pseudo-second-order and Langmuir adsorption model, and the maximum adsorption capacity is 162 mg/g. Our results proved that the TEMPO-CNF/TiO_2 nanocomposite could be used for the removal of BB from aqueous solutions.

Keywords Cellulose nanofibers · Titanium oxide · Nanocomposite · Water purification

✉ Shaymaa E. El-Shafey
s_shafey@yahoo.com

Zehbah Ali Al-Ahmed
zalshwal@kku.edu.sa

Abeer A. Hassan
ahmed.abeer91@yahoo.com

Sahar M. El-Khouly
sm6ahmedelkhouly@gmail.com

1 Department of Chemistry, College's of Art and Sciences -Dhahran Aljounb, King Khalid University, Abha, Saudi Arabia

2 Chemistry Department, Faculty of Science for Girls, Ain Shams University, Cairo, Egypt

3 Surface Chemistry and Catalysis Laboratory, Physical Chemistry Department, National Research Center, NRC, Dokki, Giza, Egypt

Introduction

Environmental contamination by organic and inorganic colorants bearing wastewater worldwide concern is required to be addressed. Various industries such as textile dying, cosmetics, pigments and paints yield a lot of fluid that contain organic colorants. These wastes are wealthy in dyes, and 10–15% of these dyes might be found in modern effluents. These organic released dyes have high toxicity, slow biodegradation [1], high resistant concerning oxidizing agents, and light and heat, and henceforth, they danger the amphibian and human life [2]. Adsorption technique has been presented as an environmentally friendly, cost-effective and easy regeneration method for the removal of heavy metals and organic dyes [3, 4]. Numerous endeavors have been cultivated to grow new practical adsorbents for lessening the grouping of the contaminants to allowable dimensions [5–7]. Polysaccharides have been modified for developing novel nanocomposite materials for water treatment. Various nanocomposites, e.g., carboxymethyl cellulose/Fe_3O_4 [8], carboxymethyl cellulose/hydroxyapatite [9], cellulose/montmorillonite [10] and graphene oxides/microcrystalline cellulose aerogels [11], have been studied for detoxification of pollutants from aqueous solutions.

Cellulose nanofibers (CNFs) with incredible physical and mechanical properties, e.g., high porosity, high versatile modulus, and high crystallinity, were emerged as an alternative non-toxic and bioactive material for preparing nanocomposites [12]. Cellulose pulp was used to prepare CNF through applying high mechanical shearing. Various pretreatment protocols were described to enable the defibrillation process such as oxidation with 2,2,6,6-tetramethylpiperidine-1-oxyl (TEMPO) which oxidizes the primary hydroxyl groups into carboxyl group [13, 14]. Moreover, mechanical shearing such as high-pressure homogenization or refining and grinding can enhance the preparation of CNF [15].

TiO_2 has recently emerged as a semiconductor photocatalyst with applications in water splitting, pollutants treatment, photovoltaics, and adsorption. It has unique properties such as chemical stability, high corrosion resistance, non-toxicity nature and low price. TiO_2 nanoparticles will in general agglomerate and lose a decent lot of surface zone which lessens their expected effectiveness for target applications. Although TiO_2 is thought to be environmentally benign, its accidental release to aquatic systems could still cause significant environmental risks. A compelling way to deal with beat the issues is to fabricate hybrid nanocomposite by immobilizing ultrafine particles onto supporting polymers, e.g., cellulose fibers. For example, Khan et al. arranged bacterial cellulose/TiO_2 nanocomposite with a wide scope of antibacterial properties. Also, the nanocomposite showed bond and expansion properties for fibroblast cells. These properties proposed the nanocomposite for restorative applications, particularly wound dressing and tissue recovery [16]. Hydroxypropyl methyl cellulose/TiO_2 hybrid nanophotocatalysts were set up by in situ combination at various weight proportions. The photocatalytic efficiency of the hybrid to degrade 4-nitrophenol was examined in aqueous medium under visible light irradiation. Comparing with pure TiO_2, the prepared nanocomposites were photocatalytically much more active and photostable after

five experimental runs [17]. In the current paper, bleached bagasse pulp was used to prepare cellulose nanofibers (CNFs). Then, CNFs/TiO_2 nanocomposite was arranged and examined as a supportable and financially smart adsorbent for the sequestration of cationic Brilliant Blue (BB) from wastewater.

Materials and methods

Materials

The raw material used in this study was bleached bagasse pulp supplied from Qena Company of Paper Industry, Egypt. 2,2,6,6-Tetramethylpiperidine-1-oxyl (TEMPO), sodium metaperiodate ($NaIO_4$), sodium bromide (NaBr), Brilliant Blue (BB) as shown in Schematic 1 and titanium (IV) isopropoxide were purchased from Sigma-Aldrich. All chemicals were used without further purification.

Preparation of TEMPO-oxidized cellulose

TEMPO-oxidized bagasse pulp was prepared as previously described [18–21]. Shortly afterward, 3 g of bleached bagasse pulp was dispersed in distilled water with TEMPO (0.048 g, 0.3 mmol) and sodium bromide 0.48 g, 4.8 mmol. Then 30 mL of sodium hypochlorite solution (15%) was added with continuous stirring, and the pH was adjusted to 10 using NaOH solution. At the end of reaction, the pH was adjusted to 7 and the product was centrifuged at 10,000 rpm several times. Finally, the product was purified by dialysis for 1 week against deionized water. TEMPO-CNF was prepared using Masuko grinder as a mechanical defibrillation treatment.

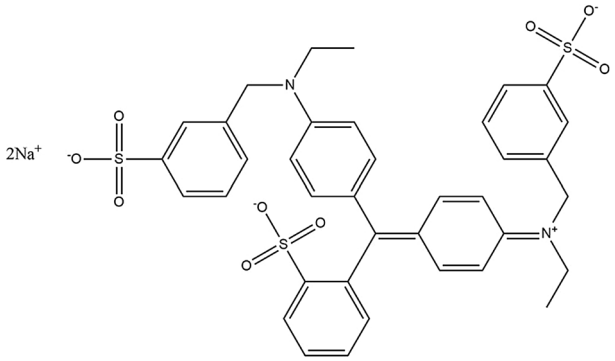

Schematic 1 The chemical structure of Brilliant Blue dye

Synthesis of TEMPO-oxidized cellules/TiO_2 nanocomposite

The synthesized TEMPO-CNF has been tested as a support sustainable polymer during TiO_2 nanoparticle precipitation [22]. In 100-mL round flask, 1 ml of titanium isopropoxide with 50 mL ethanol (analytical grade) was dropped slowly into the 5 g of the former prepared CNF under vigorous stirring at room temperature. After stirring the mixture for about 2 h, white precipitate was formed. The resulting precipitates were centrifuged, washed with distilled water, and dried in vacuum at 50 °C.

Batch adsorption studies

The prepared TEMPO-CNF/TiO_2 nanocomposite was tried as an adsorbent for dye removal. Solutions with various concentrations of BB (25–600 ppm) were prepared by stock dilution with water. BB concentration was determined colorimetrically estimating greatest absorbance at 583 nm of the arrangements by UNICO UV-2000 spectrophotometer. Set adsorption tests were led at 50 mg of TEMPO-CNF/TiO_2 and blended well with magnetic stirring and kept up for a fixed time at 25 °C. After adsorption for a definite time, pH and dye concentration, the solution was isolated and the amount of BB adsorbed at adsorption equilibrium, q_e (mg/g), was determined according to the following equation:

$$q_e = \frac{(C_o - C_e)V}{W} \tag{1}$$

where C_o and C_e are the initial and equilibrium dye concentrations (mg/L), V is the volume (L) of the dye solution used in the adsorption experiment, and W is the weight of the nanocomposite (g).

Characterization methods

The prepared samples were characterized using different types of techniques; FT-IR (Mattson 5000 FT-IR spectrometer) was done utilizing KBr disks in the range of 4000–500 cm^{-1}. Thermogravimetric analysis was done on a PerkinElmer TGA7 thermogravimetric analyzer under nitrogen. Scanning electron microscopy (SEM) was done on Model Quanta 250 FEG (field emission gun) attached with EDX unit (energy-dispersive X-ray analyses), with accelerating voltage 30 K. Transmission electron microscope (TEM) images were taken with a JEOL JEM-2100 electron microscopy.

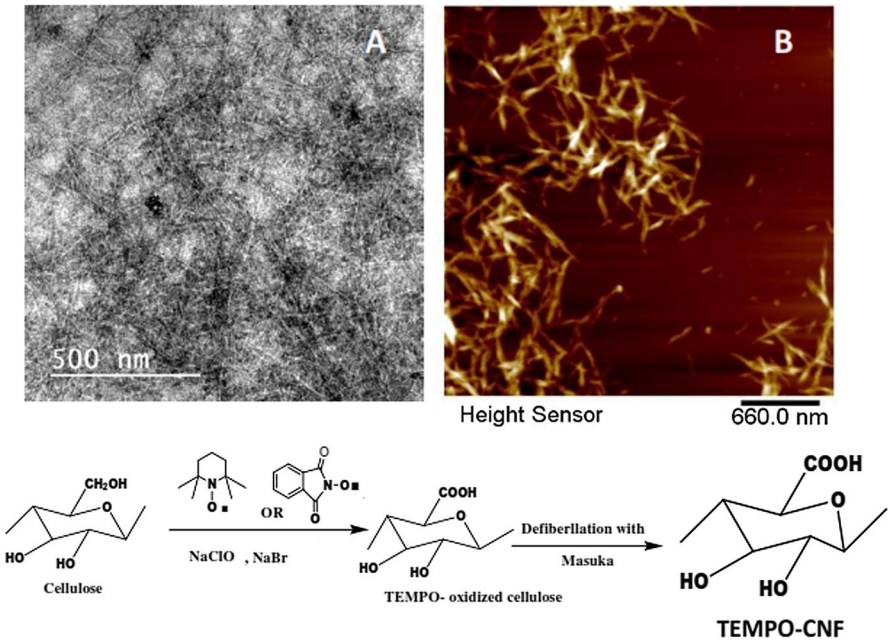

Fig. 1 **a** TEM and **b** AFM photos and the scheme of the formation of TEMPO-CNF

Results and discussion

Preparation and characterization of TEMPO-CNF

Bagasse is a main source of cellulose pulp and was reported recently as significant source for the preparation of cellulose nanofibers. Figure 1 shows the mechanism of the production of TEMPO-CNF through TEMPO-oxidation followed by mechanical defibrillation. The morphology of TEMPO-CNF was observed by means of TEM and AFM in tapping mode. Figure 1A displays the TEM and AFM analysis of TEMPO-CNF which confirms that the width of TEMPO-CNF nanofibers varies from 10 to 20 nm with several micrometers of range in length. The current results were suggested previously in our previous work and approve that TEMPO-CNF has a uniform structure because of the arrangement of carboxylate bunches on the outside of the cellulose nanofibers.

Characterizations of TEMPO-CNF/TiO_2 nanocomposite

Figure 2a shows the FT-IR spectrum of TEMPO-CNF, which displays the characteristic cellulose I bands at 3441, 2924, 1430, and 1113 cm^{-1} which apportioned to the OH, CH_2, C–H symmetrical deformation, and C–O–C stretching vibration of TEMPO-CNF, respectively [23]. The peak at 1739 cm^{-1} is assigned to stretching

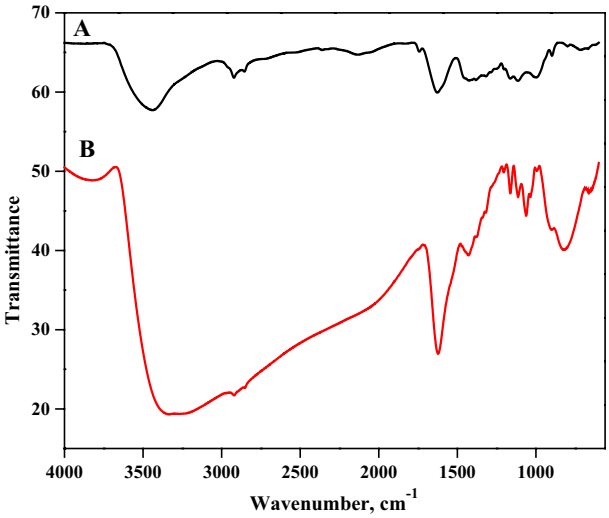

Fig. 2 FT-IR spectra of **a** TEMPO-CNF and **b** TEMPO-CNF/TiO_2 nanocomposite

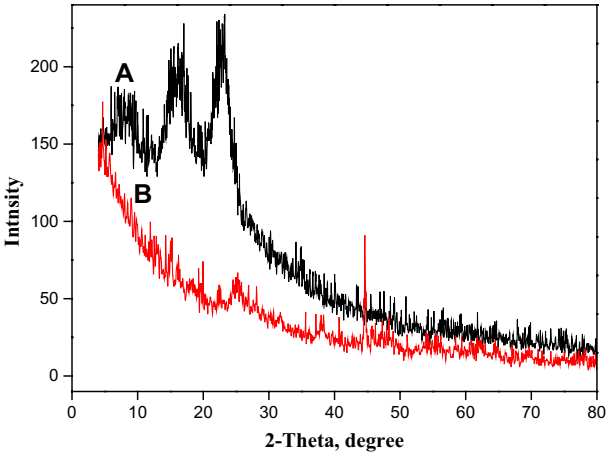

Fig. 3 XRD patterns of **a** TEMPO-CNF and **b** TEMPO-CNF/TiO_2 nanocomposite

of carbonyl groups (C=O) resulting from oxidation process. Figure 2b shows that strength of these bands was increased in the TEMPO-CNF/TiO_2 nanocomposite. The nanocomposite displays an intense band at 816 cm^{-1} and 891 cm^{-1} which assigned to the stretching vibrations of Ti–O–Ti and Ti–O.

The diffraction curves of TEMPO-CNF and TEMPO-CNF/TiO_2 nanocomposite are displayed in Fig. 3a, b. X-ray pattern of CNF gives the known diffraction peaks of cellulose I with crystalline peaks at about $2\theta = 16.2°$, 22.7°, and 34.5° which are corresponding to (1 1 0), (2 0 0), and (0 0 4) planes of crystalline

cellulose. The XRD of the TEMPO-CNF/TiO_2 nanocomposite revealed the presence of TiO_2 nanoparticles with the peaks at 2θ 24.8°, 38.25°, 44.7°, 48.3°, 54.3°, and 64°. The diffraction peaks from the treated TEMPO-CNF are not obvious in TEMPO-CNF/TiO_2 and showed poor crystallinity shifted to lower intensities. This decrease in crystallinity is due to the deposition of the TiO_2 layers on the surface of CNF by increasing the amount of TiO_2 [24]. These behaviors have been confirmed by the SEM images and also by the EDX analysis as illustrated in Fig. 5.

The thermal stability of TEMPO-CNF and TEMPO-CNF/TiO_2 nanocomposite was assessed by thermogravimetric examination (TGA). As appeared in Fig. 4, TEMPO-CNF decayed in two phases. In the begining , at 90 °C mentions to the evaporation of absorbed water on the TEMPO-CNF. Moreover, the other stage seems at 330 °C which characterizes decomposition of hydroxyl and carboxyl groups. Nevertheless, the stability of TEMPO-CNF/TiO_2 nanocomposite is higher compared to TEMPO-CNF. At 700 °C, TEMPO-CNF and TEMPO-CNF/TiO_2 nanocomposite show residual weights 24.1 and 73%.

The morphology of TEMPO-CNF and TEMPO-CNF/TiO_2 was explored utilizing SEM and EDX analysis as displayed in Fig. 5. TEMPO-CNF shows fiber structure with different widths. TEMPO-CNF/TiO_2 nanocomposite showed spherical shape. Moreover, the SEM image signifies that the nanocomposite displays accumulation as a result of TiO_2 homogenously mixed with TEMPO-CNF. Also, TiO_2 nanoparticles give off an impression to be more distinct and uniform, likely because of the combination between TEMPO-CNF and TiO_2 nanoparticles that reduces the attractive forces between TiO_2, decreasing their aggregation affinity. The EDX results reveal that the TiO_2 is mainly composed of C, O, and Ti. It was observed clearly that the main surface atomic ratio is for Ti, confirming the formation of TiO_2 on the surface than that the bulk of the nanocomposite.

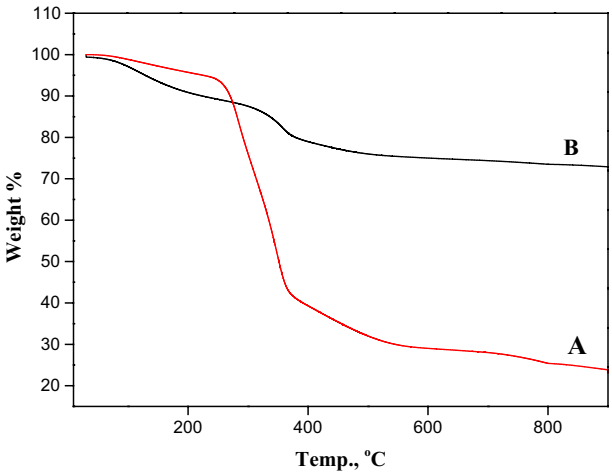

Fig. 4 TGA analysis of **a** TEMPO-CNF and **b** TEMPO-CNF/TiO_2 nanocomposite

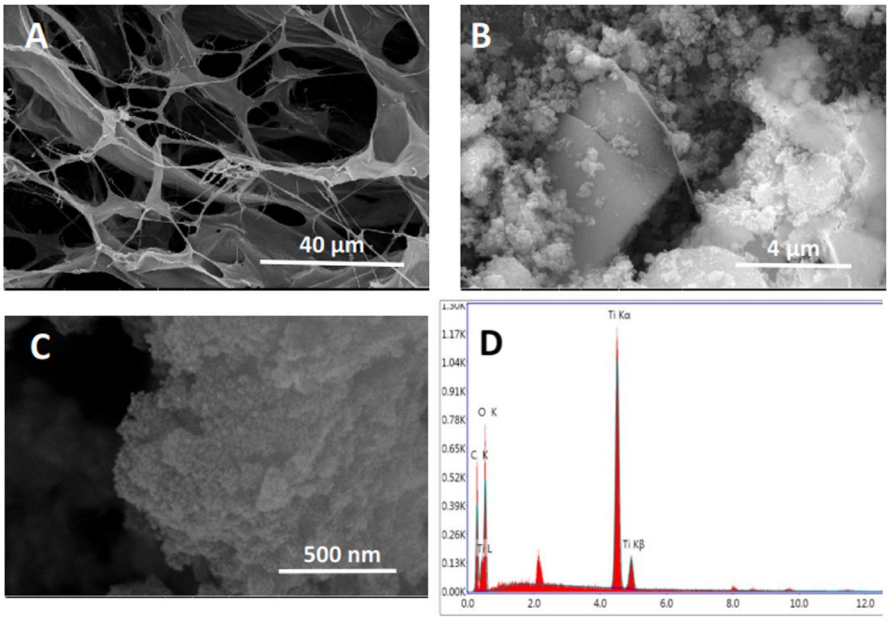

Fig. 5 SEM images of **a** TEMPO-CNF, **b** and **c** TEMPO-CNF/TiO_2 nanocomposite, and **d** EDX of the nanocomposite

Application of TEMPO-CNF/TiO_2 nanocomposite for BB adsorption

The prepared TEMPO-CNF/TiO_2 nanocomposite was explored for the removal of BB from aqueous solutions. Various parameters were examined to calculate the

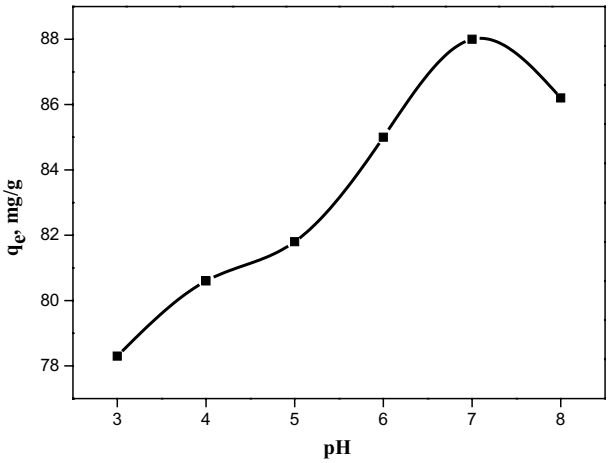

Fig. 6 Effect of the pH on the capacities of TEMPO-CNF/TiO_2 nanocomposite for BB. Adsorption experiments: BB concentration 50 mg/L; oxidized cellulose 0.05 g/50 mL, and contact time 60 min)

potential of the TEMPO-CNF/TiO_2 nanocomposite as an adsorbent for cationic dyes.

Effect of pH

The adsorption capacity of TEMPO-CNF/TiO_2 nanocomposite with pH change was examined as shown in Fig. 6. The displayed results showed that the adsorption of BB gradually increased to reach the optimum value at pH 7. The adsorption capacity recorded 88 mg/g for TEMPO-CNF/TiO_2 nanocomposite. At low pH, the functional groups in the TEMPO-CNF/TiO_2 nanocomposite were protonated and existed as positively charged groups. The electrostatic repulsions between BB and these groups may inhibit the adsorption process [25]. The isoelectric purpose of TiO_2 was 5.1. Thus, at pH higher than 5.1, the TiO_2 surface would remain contrarily charged. However, the BB removal limit was diminished at pH higher than 6 [26]. This performance proved the role of TiO_2 nanoparticles for improving the adsorption performance of the nanocomposite which represent additional sites for electrostatic interactions with cationic BB molecules.

In addition, the pH results showed the neutral solution is favored for the development of the adsorption limit of the TEMPO-CNF/TiO_2 nanocomposite. Expanding the adsorption ability of cationic dyes with pH has been portrayed in past investigations [27].

Effect of contact time

The rate of BB uptake depends on the contact time between TEMPO-CNF/TiO_2 nanocomposite and the dye solution [28]. Variation of time was studied in range from 5 to 240 min with 0.05 g of adsorbent at pH 7. The adsorption capacity of

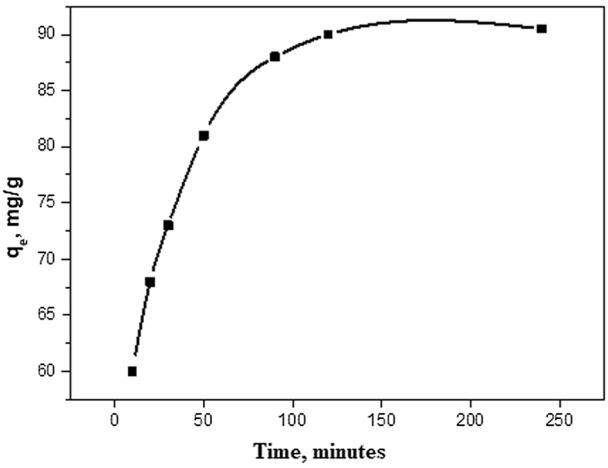

Fig. 7 Effect of time on capacity of TEMPO-CNF/TiO_2 nanocomposite for BB adsorption: BB concentration: 50 mg/L; nanocomposite: 0.05 g/50 mL, and pH: 7

Table 1 Kinetic parameters for BB adsorption by TEMPO-CNF/TiO_2 nanocomposite

Pseudo-first-order model				Pseudo-second-order model		
$q_{e,exp}$ (mg/g)	$q_{e,cal}$ (mg/g)	K_1 (min^{-1})	R^2	$q_{e,cal}$ (mg/g)	K_2 (g mg^{-1} min^{-1})	R^2
90.5	26	0.0092	0.732	93	1.6×10^{-3}	0.999

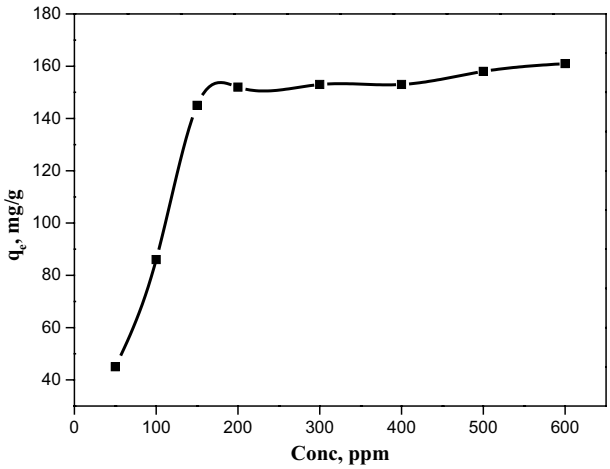

Fig. 8 Effect of BB content on the adsorption capacity of TEMPO-CNF/TiO_2 nanocomposite. Adsorption experiments: content of nanocomposite: 0.05 g/50 mL; pH: 7, and contact time 80 min

BB on TEMPO-CNF/TiO_2 nanocomposite was increased gradually through the first 60 min and reached a plateau after 80 min as displayed in Fig. 7.

The pseudo-first- and pseudo-second-order models are shown in Eqs. (2 and 3), respectively.

$$\log(q_e - q_t) = \log(q_e) - \frac{K_1}{2.303}t \tag{2}$$

$$\frac{t}{q_t} = \frac{t}{q_e} + \frac{1}{k_2 q_{e2}} \tag{3}$$

The parameters of the kinetic models for TEMPO-CNF/TiO_2 nanocomposite are displayed in Table 1. The calculated correlation coefficients (R^2), for the nanocomposite, reported that the adsorption of BB followed the pseudo-second-order model. These results suggest that the chemical bonds between BB and TEMPO-CNF/TiO_2 nanocomposite controlled the adsorption.

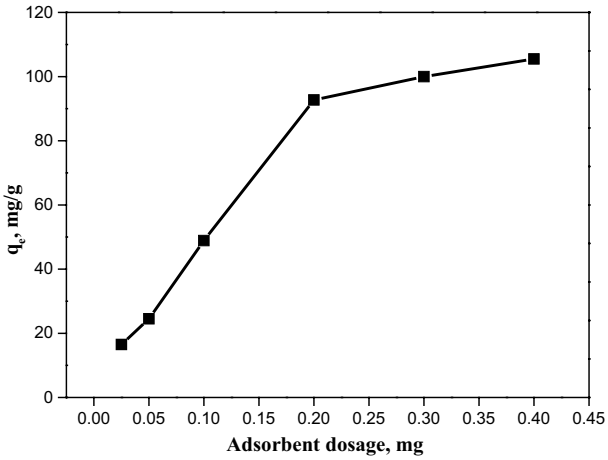

Fig. 9 Effect of TEMPO-CNF/TiO_2 content on the adsorption capacity of BB dye. Adsorption experiments: dye concentration 200 mg/L; pH: 7 and contact time 80 min

Influence of initial BB concentration

Figure 8 proves the effect of BB content on the adsorption process of TEMPO-CNF/TiO_2 nanocomposite. BB elimination increases gradually up to 152 mg/g at BB content 200 ppm. The adsorption capacity tends to levels off with higher concentrations.

Effect of dose of TEMPO-CNF/TiO_2 nanocomposite

Different doses of TEMPO-CNF/TiO_2 nanocomposite ranging from 0.025 to 0.5 mg/L with 50 mL of dye (200 mg/L) were used to evaluate the adsorption capacity at optimum condition of pH and contact time 80 min at 25 °C. Figure 9 shows that the adsorption process increases by increasing the adsorbent dose until reaching the maximum value with 0.2 g/50 mL dose of the studied dye. By increasing the adsorbent content, there is no remarkable increase in the adsorption process. This increasing in the dye uptake with the adsorbent dose can be attributed to the increase in the number of adsorption sites [29].

Isotherm models

The Langmuir isotherm parameters are calculated from Eq. 4: [30]

Table 2 Parameters for BB adsorption by TEMPO-CNF/TiO_2 nanocomposite according to different equilibrium models

Langmuir isotherm constants			Freundlich isotherm constants		
K_s (mg/L)	q_m (mg/g)	R^2	P (mg/g)	n	R^2
8.38	162	0.998	63	6.01	0.59

Table 3 Maximum adsorption of various cellulose composite materials

Adsorbent	Maximum adsorption (mg/g)	Organic dye	References
Cellulose-grafted SPI/hydroxyapatite hybrid	454	MB	[32]
Cellulose/chitosan aerogel	382	Congo red	[33]
Cellulose nanocrystal/alginate	256	MB	[34]
Carboxymethyl cellulose-g-polymethacrylic acid/calcium phosphate	180	MB	[35]
TiO_2/activated carbon	80%	BB	[36]
Our nanocomposite	162	BB	This work

MB methylene blue dye, *BB* Brilliant Blue dye

$$\frac{C_e}{q_e} = \frac{K_s}{q_{max}} + \frac{C_e}{q_{max}} \tag{4}$$

where C_e (mg L^{-1}) is the concentration at equilibrium, q_e (mg g^{-1}) is the amount adsorbed at equilibrium, q_{max} (mg g^{-1}) is the maximum quantity adsorbed, and K_s (L mg^{-1}) is the Langmuir isotherm constant. Two lines are obtained by plotting $1/q_e$ as a function of $1/C_e$ in the concentration range studied of the dye. The correlation coefficient of BB adsorption is calculated and presented in Table 2. The high values of correlation coefficients ($R^2 > 0.998$) illustrate that the Langmuir equation agrees with BB adsorption on TEMPO-CNF/TiO_2 nanocomposite. The parameter q_{max} recorded the value of 162 mg/g.

The Freundlich model is represented in Eq. 5: [31]

$$\log q_e = \frac{1}{n} \log C_e + \log P \tag{5}$$

where C_e is the equilibrium concentration (mg/L) and P is Freundlich constants (mg/g $(L/mg)^{1/n}$) related to the adsorption capacity and $1/n$ is the adsorption intensity. Freundlich constants P and $1/n$ can be calculated from the intercept and slope of the linear plot with log q_e against log C_e.

The low value of the linear coefficient for Freundlich model (0.59) was recorded. Moreover, the values of P and n consonants are 63 and 6.01 for TEMPO-CNF/TiO_2 nanocomposite. These results proved that this model is not appropriate for the adsorption of BB onto the prepared nanocomposite.

A comparison between TEMPO-CNF/TiO_2 nanocomposites with other adsorbents toward BB adsorption is presented in Table 3. TEMPO-CNF/TiO_2 nanocomposite had high BB adsorption compared with other cellulosic materials reported in previous studies.

Conclusion

A TEMPO-CNF/TiO_2 nanocomposite was prepared from bleached bagasse pulp after TEMPO-oxidation steps. SEM observation exhibited that TiO_2 in the range of 10 nm. The adsorption capacity of TEMPO-CNF/TiO_2 nanocomposites for BB is favorable at slight alkaline medium. BB adsorption onto TEMPO-CNF/TiO_2 nanocomposites is well described by pseudo-second-order and Langmuir isotherm with the adsorption capacity of 162 mg/g. This work provides an alternative biocompatible adsorbent, TEMPO-CNF/TiO_2 nanocomposite, with the adsorption ability for organic pollutants.

Acknowledgements The authors extend their appreciation to Dr. Ragab Abou-Zeid from Cellulose and Paper Department, National Research Center, for supporting this work through preparation of CNF.

Compliance with ethical standards

Conflict of interest The authors declare that they have no conflict of interest.

References

1. Niu P, Hao J (2011) Fabrication of titanium dioxide and tungstophosphate nanocomposite films and their photocatalytic degradation for methyl orange. Langmuir 27:13590–13597
2. Haque E, Jun JW, Jhung SH (2011) Adsorptive removal of methyl orange and methylene blue from aqueous solution with a metal-organic framework material, iron terephthalate (MOF-235). J Hazard Mater 185:507–511
3. Salama A (2018) Preparation of CMC-g-P(SPMA) super adsorbent hydrogels: exploring their capacity for MB removal from waste water. Int J Biol Macromol 106:940–946
4. Salama A, Shoueir KR, Aljohani HA (2017) Preparation of sustainable nanocomposite as new adsorbent for dyes removal. Fibers Polym 18:1825–1830
5. Salama A, Shukry N, El-Sakhawy M (2015) Carboxymethyl cellulose-g-poly(2-(dimethylamino) ethyl methacrylate) hydrogel as adsorbent for dye removal. Int J Biol Macromol 73:72–75
6. Salama A, Hesemann P (2018) Synthesis of N-guanidinium-chitosan/silica hybrid composites: efficient adsorbents for anionic pollutants. J Polym Environ 26:1986–1997
7. Monier M, Ayad DM, Wei Y (2010) Adsorption of Cu(II), Co(II), and Ni(II) ions by modified magnetic chitosan chelating resin. J Hazard Mater 177:962–970
8. Salama A, Etri S, Mohamed SAA (2018) Carboxymethyl cellulose prepared from mesquite tree: new source for promising nanocomposite materials. Carbohydr Polym 189:138–144
9. Manatunga DC, de Silva RM, de Silva KMN (2016) Natural polysaccharides leading to super adsorbent hydroxyapatite nanoparticles for the removal of heavy metals and dyes from aqueous solutions. RSC Adv. 6:105618–105630
10. Kumar ASK, Kalidhasan S, Rajesh V et al (2012) Application of cellulose-clay composite biosorbent toward the effective adsorption and removal of chromium from industrial wastewater. Ind Eng Chem Res 51:58–69
11. Wei X, Huang T, Yang JH (2017) Green synthesis of hybrid graphene oxide/microcrystalline cellulose aerogels and their use as superabsorbents. J Hazard Mater 335:28–38
12. Lavoine N, Desloges I, Dufresne A (2012) Microfibrillated cellulose—its barrier properties and applications in cellulosic materials: a review. Carbohydr Polym 90:735–764
13. Saini S, Sillard C, Naceur Belgacem M (2016) Nisin anchored cellulose nanofibers for long term antimicrobial active food packaging. RSC Adv. 6:12422–12430
14. Abo-uzeid RE, Khiari R, Beneventi D (2018) Biomimetic mineralization of three-dimensional printed alginate/TEMPO-oxidized cellulose nanofibril scaffolds for bone tissue engineering. Biomacromol 19:4442–4452
15. Abou-Zeid RE, Khiari R, El-Wakil N (2018) Current state and new trends in the use of cellulose nanomaterials for wastewater treatment. Biomacromol. https://doi.org/10.1021/acs.biomac.8b00839

16. Khalid A, Ullah H, Ul-Islam M (2017) Bacterial cellulose–TiO_2 nanocomposites promote healing and tissue regeneration in burn mice model. RSC Adv. 7:47662–47668
17. Nsib MF, Hajji F, Mayoufi A (2014) In situ synthesis and characterization of TiO_2/HPM cellulose hybrid material for the photocatalytic degradation of 4-NP under visible light. Comptes Rendus Chim. 17:839–848
18. Saito T, Uematsu T, Kimura S (2011) Self-aligned integration of native cellulose nanofibrils towards producing diverse bulk materials. Soft Matter 7:8804
19. Abou-Zeid RE, Dacrory S, Ali KA, Kamel S (2018) Novel method of preparation of tricarboxylic cellulose nanofiber for efficient removal of heavy metal ions from aqueous solution. Int J Biol Macromol 119:207–214
20. El-Gendy A, Abou-Zeid RE, Salama A, Diab M (2017) TEMPO-oxidized cellulose nanofibers/polylactic acid/TiO_2 as antibacterial bionanocomposite for active packaging. Egypt J Chem 60:1007–1014
21. Hassan M, Berglund L, Hassan E, Abou-Zeid R, Oksman K (2018) Effect of xylanase pretreatment of rice straw unbleached soda and neutral sulfite pulps on isolation of nanofibers and their properties. Cellulose 25:2939–2953
22. Ngenefeme JF-T, Eko JN, Mbom DYA (2013) One pot green synthesis and characterisation of iron oxide-pectin hybrid nanocomposite. Open J Compos Mater. 03:30–37
23. Salama A, Neumann M, Günter C (2014) Ionic liquid-assisted formation of cellulose/calcium phosphate hybrid materials. Beilstein J Nanotechnol. 5:1553–1568
24. El-Kemary MA, El-mehasseb IM, Shoueir KR, El-Shafey SE, El-Shafey OI, Aljohani HA, Fouad RR (2018) Sol–gel TiO_2 decorated on eggshell nanocrystal as engineered adsorbents for removal of acid dye. J Disper Sci Technol 39:911–921
25. Monier M, Abdel-Latif DA (2012) Preparation of cross-linked magnetic chitosan-phenylthiourea resin for adsorption of Hg(II), Cd(II) and Zn(II) ions from aqueous solutions. J Hazard Mater 209–210:240–249
26. Mohammadi A, Karimi AA (2017) Methylene blue removal using surface-modified TiO_2 nanoparticles: a comparative study on adsorption and photocatalytic degradation. J Water Environ Nanotechnol. 2:118–128
27. Zhao R, Wang Y, Li X (2015) Synthesis of β-cyclodextrin-based electrospun nanofiber membranes for highly efficient adsorption and separation of methylene blue. ACS Appl Mater Interfaces 7:26649–26657
28. Ma J, Yu F, Zhou L (2012) Enhanced adsorptive removal of methyl orange and methylene blue from aqueous solution by alkali-activated multiwalled carbon nanotubes. ACS Appl Mater Interfaces 4:5749–5760
29. Khoshhesab Z, Gonbadi K, Behbehani G (2015) Removal of reactive black 8 dye from aqueous solutions using zinc oxide nanoparticles: investigation of adsorption parameters. Desalination and Water Treatment 56:1558–1565
30. Langmuir I (1918) The adsorption of gases on plane surfaces of glass, mica and platinum. J Am Chem Soc 40:1361
31. Freundlich HMF (1906) Over the adsorption in solution. J Phys Chem 57:385–470
32. Salama A (2017) New sustainable hybrid material as adsorbent for dye removal from aqueous solutions. J Colloid Interface Sci 487:348–353
33. Wang Y, Wang H, Peng H (2018) Dye adsorption from aqueous solution by cellulose/chitosan composite: equilibrium, kinetics, and thermodynamics. Fibers Polym. 19:340–349
34. Mohammed N, Grishkewich N, Berry RM (2015) Cellulose nanocrystal–alginate hydrogel beads as novel adsorbents for organic dyes in aqueous solutions. Cellulose 22:3725–3738
35. Salama A (2016) Functionalized hybrid materials assisted organic dyes removal from aqueous solutions. Environ Nanotechnology, Monit Manag. 6:159–163
36. Geng Qijin, Cui Wenwen (2010) Adsorption and photocatalytic degradation of reactive brilliant red K-2BP by TiO_2/AC in bubbling fluidized bed photocatalytic reactor. Ind Eng Chem Res 49:11321–11330